In Vitro Phosphorylation of Insulin Receptor Substrate 1 by Protein Kinase C-ζ: Functional Analysis and Identification of Novel Phosphorylation Sites†

Mark R. Sommerfeld,‡ Sabine Metzger,§ Magdalene Stosik,‡ Norbert Tennagels,|| and Jürgen Eckel*,‡

Department of Clinical Biochemistry and Pathobiochemistry, German Diabetes Research Institute, and Biomedical Research Centre, Heinrich-Heine-University, Düsseldorf, Germany, and Aventis Pharma, Frankfurt, Germany

Received February 18, 2004

ABSTRACT: Protein kinase C-ζ (PKC-ζ) participates both in downstream insulin signaling and in the negative feedback control of insulin action. Here we used an in vitro approach to identify PKC-ζ phosphorylation sites within insulin receptor substrate 1 (IRS-1) and to characterize the functional implications. A recombinant IRS-1 fragment (rIRS-1$^{449-664}$) containing major tyrosine motifs for interaction with phosphatidylinositol (PI) 3-kinase strongly associated to the p85α subunit of PI 3-kinase after Tyr phosphorylation by the insulin receptor. Phosphorylation of rIRS-1$^{449-664}$ by PKC-ζ induced a prominent inhibition of this process with a mixture of classical PKC isoforms being less effective. Both PKC-ζ and the classical isoforms phosphorylated rIRS-1$^{449-664}$ on Ser^{612}. However, modification of this residue did not reduce the affinity of p85α binding to pTyr-containing peptides (amino acids 605−615 of rat IRS-1), as determined by surface plasmon resonance. rIRS-1$^{449-664}$ was then phosphorylated by PKC-ζ using [^{32}P]ATP and subjected to tryptic phosphopeptide mapping based on two-dimensional HPLC coupled to mass spectrometry. Ser^{498} and Ser^{570} were identified as novel phosphoserine sites targeted by PKC-ζ. Both sites were additionally confirmed by phosphopeptide mapping of the corresponding Ser → Ala mutants of rIRS-1$^{449-664}$. Ser^{570} was specifically targeted by PKC-ζ, as shown by immunoblotting with a phosphospecific antiserum against Ser^{570} of IRS-1. Binding of p85α to the S570A mutant was less susceptible to inhibition by PKC-ζ, when compared to the S612A mutant. In conclusion, our in vitro data demonstrate a strong inhibitory action of PKC-ζ at the level of IRS-1/PI 3-kinase interaction involving multiple serine phosphorylation sites. Whereas Ser^{612} appears not to participate in the negative control of insulin signaling, Ser^{570} may at least partly contribute to this process.

Insulin receptor substrate (IRS)[1] proteins are phosphorylated on multiple tyrosine residues by the activated insulin receptor and play a pivotal role in the process of downstream insulin signaling (*1*, *2*). The phosphotyrosine motifs, specifically within IRS-1 and IRS-2, serve as docking sites for a series of adaptor proteins that possess src homology 2 (SH2) domains including Grb2, the intracellular PTPase SHP-2, Nck, Crk, and phosphatidylinositol 3-kinase (PI 3-kinase) (*3*−*5*). PI 3-kinase is composed of a catalytic 110 kDa subunit (p110) and a regulatory 85 kDa subunit (p85) containing two SH2 domains that bind to tyrosine-phosphorylated pYMXM and pYXXM motifs in IRS proteins and induce PI 3-kinase activation (*6*). This leads to stimulation of additional downstream kinases including the serine/threonine kinase PKB/Akt (*7*, *8*) and the atypical protein kinase C isoforms ζ and λ (PKC-ζ/λ) (*9*, *10*) by phosphoinositide-dependent kinase 1. Activation of PKB and PKC-ζ/λ and its downstream signals have been shown to play a critical role in mediating the metabolic actions of insulin such as GLUT4 translocation and glucose transport (*9*, *10*), GSK3 serine phosphorylation and glycogen synthesis (*11*), PDE serine phosphorylation and antilipolysis (*12*, *13*), and mTOR activation and protein synthesis (*14*, *15*).

Dysregulation of the insulin-signaling system is a multifactorial process leading to insulin resistance and type 2 diabetes with the IRS proteins potentially representing a major target (*16*). Thus, serine/threonine phosphorylation of IRS proteins has been proposed to play a key role both in feedback inhibition of the insulin signal and in the development of cellular insulin resistance (for review, see refs *16*−*18*). Covalent modification of IRS-1 on serine/threonine was shown to impair its insulin-induced tyrosine phosphorylation, the activation of PI 3-kinase, and the stimulation of glucose transport (*19*). In the unstimulated state serine/threonine phosphorylation of IRS-1 occurs constitutively in the cell (*20*), and it is further promoted by cytokines and metabolites

† This work was supported by the Ministerium für Wissenschaft und Forschung des Landes Nordrhein-Westfalen, by the Bundesministerium für Gesundheit, EU COST Action B 17, and by a grant from Aventis Pharma, Frankfurt, Germany.

* To whom correspondence should be addressed. Tel: +492113382561. Fax: +492113382582. E-mail: eckel@uni-duesseldorf.de.

‡ German Diabetes Research Institute.

§ Biomedical Research Centre, Heinrich-Heine-University.

|| Aventis Pharma.

[1] Abbreviations: GST, glutathione *S*-transferase; HPLC, high-performance liquid chromatography; IR, insulin receptor; IRS, insulin receptor substrate; ESI-MS, electrospray ionization mass spectrometry; p85, regulatory subunit of phosphatidylinositol (PI) 3-kinase; PAGE, polyacrylamide gel electrophoresis; PI 3-kinase, phosphatidylinositol 3-kinase; RP, reversed phase; PKC, protein kinase C; PKB, protein kinase B; RTKs, receptor tyrosine kinases; SH2, src homology domain 2; WGA, wheat germ agglutinin; SDS, sodium dodecyl sulfate; ECL, enhanced chemiluminescence.

10.1021/bi049640v CCC: $27.50
Published on Web 04/16/2004

that inhibit signal transduction like tumor necrosis factor (TNF) α (*21*), free fatty acids, glucose, or ceramide (*22*). Furthermore, hyperphosphorylation of IRS-1 on serine/threonine residues is a common finding during insulin resistance and type 2 diabetes (*23*).

Despite a key role for the development of insulin resistance, the serine phosphorylation of IRS-1 has remained incompletely understood, mainly because IRS-1 contains more than 100 potential serine phosphorylation sites and because it was shown to represent a substrate for many protein kinases including c-Jun N-terminal kinase (JNK) (*24*), IκB kinase β (*25*), MAP kinase (*26*), protein kinase B (PKB) (*27*), and AMP-activated protein kinase (AMPK) (*28*). Interestingly, both PKB and AMPK were found to operate as a positive regulator of IRS-1 function, supporting the notion that serine/threonine phosphorylation of IRS-1 has a dual role, either to enhance or to terminate insulin signaling (*29*). Identification of residues within different domains of IRS-1 undergoing serine phosphorylation in response to different stimuli has improved our understanding of this highly complex regulatory step in insulin action. Thus, Ser^{307}, which is located near the phosphotyrosine-binding (PTB) domain, has been identified as a target for stress-activated kinases including JNK (*24*) and may also play a role as a negative feedback regulator of insulin action (*30*). Ser^{789} is targeted by AMPK and positively modulates insulin action (*28*); however, Ser^{789} phosphorylation by unidentified kinases was also found to attenuate insulin signaling (*31*). Ser^{612}, Ser^{632}, Ser^{662}, and Ser^{731} are located within or near the PI 3-kinase interaction domain; however, the functional implications of these sites have remained elusive (*32*−*34*).

In contrast to the protein kinases mentioned above, protein kinase C (PKC) ζ, which is an atypical member of the PKC family of serine/threonine kinases, appears to participate both in the downstream transduction of the insulin signal and in the negative feedback control of IRS-1 function (*10*, *35*−*38*). Thus, PKC-ζ was found to colocalize with GLUT4 and to be essential for insulin-regulated GLUT4 translocation and glucose transport in skeletal muscle (*35*) and adipocytes (*10*). Further, defective activation of PKC-ζ may contribute to obesity-dependent development of skeletal muscle insulin resistance (*36*). Recent data by Quon and co-workers (*37*) have shown that IRS-1 represents a novel substrate for PKC-ζ, and in a parallel study Zick and co-workers (*38*) found that this process inhibits PI 3-kinase activation, suggesting that PKC-ζ represents a key element in the negative feedback control of insulin action. The critical serine/threonine phospho sites mediating this process are presently not known. In the present investigation we have used an in vitro approach to identify serine/threonine phosphorylation sites for PKC-ζ within IRS-1 and to characterize the functional implications. Specifically, we have used here a recombinant IRS-1 domain comprising 216 amino acids from positions 449 to 664 (rIRS-$1^{449-664}$). This domain contains Tyr^{608} and Tyr^{628}, which are of primary importance for full activation of PI 3-kinase and GLUT4 translocation (*39*). Our results show a prominent inhibition of IRS-1/PI 3-kinase interaction by PKC-ζ most likely involving multiple phosphorylation sites. Ser^{612}, Ser^{498}, and Ser^{570} are phosphorylated by PKC-ζ, with the latter representing a novel phosphorylation site with potential functional implications.

EXPERIMENTAL PROCEDURES

Materials. Oligonucleotide primers were obtained from MWG-Biotech (Ebersberg, Germany). BL21 Codon Plus and the QuikChange site-directed mutagenesis kit were purchased from Stratagene (La Jolla, CA). One Shot TOP 10 competent cells were from Invitrogen (Karlsruhe, Germany). A plasmid miniprep kit was obtained from Qiagen (Hilden, Germany). A polyclonal anti-IRS-1 antiserum was a gift from Dr. J. A. Maassen (Leiden, The Netherlands). Anti-phosphotyrosine antibody (RC20) coupled to horseradish peroxidase and anti-p85α antibody were obtained from Transduction Laboratories, Inc. (Lexington, KY). Monoclonal anti-IRβ antibody was supplied from Oncogene (Cambridge, MA). Anti-IRS-1 pS616 antibody was from Biosource (Camarillo, CA). Anti-IRS-1 pS570 antibody was generated by immunizing rabbits with the peptide Cys-PGYRH(pS)AFVPTH and was provided by Aventis (Frankfurt, Germany). HRP-conjugated anti-rabbit and anti-mouse IgG antibody as secondary antibody for enhanced chemiluminescence (ECL) detection was from Promega Corp. (Mannheim, Germany). Protein kinase C from rat brain (PKC-rb), recombinant human protein kinase C-ζ, bisindolylmaleimide I (BIM), and PKC-ζ pseudosubstrate inhibitor were obtained from Calbiochem (San Diego, CA). α-Thrombin was purchased from Upstate Biotechnology Inc. (Lake Placid, NY). Enzymes for molecular biology, Complete protease inhibitor cocktail, and modified trypsin, sequencing grade, were obtained from Roche (Mannheim, Germany). Okadaic acid, phosphatidylserine, and wheat germ agglutinin (*Triticum vulgaris*) were purchased from Sigma (München, Germany). IRS-1 peptides were synthesized by Dr. Hoffmann (BMFZ, University of Düsseldorf, Düsseldorf, Germany). Chemicals for SDS−PAGE, GST gene fusion vector pGEX-5X-3, glutathione−Sepharose 4B, and [γ-^{32}P]ATP were supplied by Amersham Biosciences (Freiburg, Germany). GelCode Blue Stain reagent, Restore Western blot stripping buffer, and SuperSignal substrate was obtained from Pierce (Rockford, IL). BIAcore X and sensor chip CM5 are products of Biacore (Freiburg, Germany). All other chemicals were of the highest grade commercially available.

Construction and Expression of Fusion Proteins. The regulatory p85α subunit of bovine PI 3-kinase cloned into the expression vector pGEX-2T was a kind gift of Dr. P. Shepherd (London, U.K.). A glutathione *S*-transferase (GST) fusion protein containing amino acids 449−664 of rat IRS-1 (rIRS-$1^{449-664}$, molecular mass of 51.2 kDa) was prepared on the basis of the method described by Smith and Johnson (*40*) using the pGEX-5X-3 vector. Corresponding rat cDNA was generated from RNA isolated from rat heart by reverse transcription using avian myeloblastosis virus reverse transcriptase and subsequent amplification by polymerase chain reaction using Pwo DNA polymerase and the following oligonucleotide primers: 5′-primer, ATATTGTCGACCACACCCCACCAGCCAGG; 3′-primer, ATGTACTACTACAGAGGGTCACGCCGGCGTAAGAATA. The PCR products were isolated, digested with appropriate restriction enzymes, and subcloned into pGEX-5X-3. The identity of the rat IRS-1 clone was verified by restriction endonuclease analysis and nucleotide sequencing. This vector and the p85α-pGEX-2T construct were used to transform *Escherichia coli* BL21. Transformed cells were grown to an A_{600nm}

of 0.6−0.8 in 2× YTA medium (16 g/L tryptone, 10 g/L yeast, 5 g/L NaCl) supplemented with 0.1 mg/mL ampicillin and induced for 2 h with 0.1 mM isopropyl β-D-thiogalactoside (IPTG). Fusion proteins were purified by affinity chromatography on glutathione−Sepharose columns and eluted by 10 mM glutathione in 50 mM Tris-HCl (pH 8.0). The GST part of the p85α GST fusion protein was proteolytically removed using bovine thrombin in PBS. The protease was added to the fusion protein bound to the glutathione−Sepharose column and incubated for 2 h at room temperature, and then the eluate was collected. Protein content was determined using a modification of the Bio-Rad protein assay. All GST fusion proteins had the expected molecular mass when analyzed by sodium dodecyl sulfate (SDS)−polyacrylamide gel electrophoresis (PAGE).

Insulin Receptor Kinase Preparation. Rat liver was rapidly removed, immediately frozen in liquid nitrogen, and processed as described (*41*). Briefly, 3.5 vol/wt of an ice-cold buffer consisting of 50 mM Hepes (pH 7.4), 1% Triton X-100, and 2× Complete protease inhibitors was added, and the liver was homogenized using an Ultraturrax and a Potter-Elvehjem homogenizer, followed by centrifugation at 10000*g* for 10 min at 4 °C. The resultant supernatant was slowly stirred at room temperature for 60 min and then again centrifuged at 100000*g* for 90 min at 4 °C. The supernatant was then applied to an agarose-bound wheat germ agglutinin (WGA) column. The column was washed with 50 mM Hepes (pH 7.4) and 0.1% Triton X-100, and bound glycoproteins were eluted from the WGA column with this buffer containing 0.3 M *N*-acetylglucosamine.

In Vitro Phosphorylation Assay. For rIRS-1$^{449-664}$ phosphorylation by insulin receptor, 5 μg of the WGA-purified glycoprotein fraction was preincubated for 30 min at 30 °C with 100 nM insulin in a phosphorylation buffer containing 20 mM Hepes (pH 7.4), 1 mM DTT, 10 mM $MgCl_2$, 100 μg/mL bovine serum albumin, 0.2 mM Na_3VO_4, 1.7 mM $CaCl_2$, 0.6 mg/mL phosphatidylserine, and 0.5 μg/mL okadaic acid. Autophosphorylation was initiated by the addition of ATP at a concentration of 50 μM and continued for 10 min at 30 °C. Substrate phosphorylations were initiated by addition of equal volumes of rIRS-1$^{449-669}$ (1 μg) with or without pretreatment (30 min) by the PKC isoforms in the same buffer in the presence of 50 μM ATP and were allowed to proceed for 10 min at 30 °C in a final volume of 50 μL. The reaction was terminated by the addition of 6× sample buffer [0.35 M Tris-HCl (pH 6.8), 10.28% (w/v) SDS, 36% (v/v) glycerol, 0.6 M DTT, 0.012% (w/v) bromphenol blue] and boiling for 5 min. Proteins were separated by SDS−PAGE and analyzed by immunodetection with an anti-phosphotyrosine antibody after transfer to nitrocellulose. Serine/threonine phosphorylation of rIRS-1$^{449-664}$ by different PKC isoforms was assessed by incubating 1 μg of rIRS-1$^{449-664}$ with 0.5 μg of PKC-rb or PKC-ζ in phosphorylation buffer for 30 min at 30 °C in the presence of 50 μM ATP plus 2 μCi of [γ-^{32}P]ATP in a volume of 20 μL. Proteins were resolved by SDS−PAGE, and the stained and dried gels were subjected to autoradiography. The extent of phosphate incorporation was determined by Cerenkov counting of excised fragments.

GST Pull-Down Assay. In vitro phosphorylated rIRS-1$^{449-664}$ was incubated with glutathione−Sepharose beads on a rotator for 1 h at 4 °C. Pellets were washed three times with binding buffer [50 mM Tris-HCl (pH 7.4), 150 mM NaCl, 1% (v/v) Nonidet P-40, 1 mM EDTA, 1 mM NaF, 1 mM Na_3VO_4]. Then 0.5 μg of recombinant p85α was added, and incubation was continued for 2 h at 4 °C. After washing three times, the bound proteins were eluted with 20 μL of 2× sample buffer and separated by SDS−PAGE.

Immunoblotting. Proteins were separated by SDS−PAGE using 8−18% gradient gels, followed by transfer to nitrocellulose in a semidry blotting apparatus. The membrane was then blocked for 60 min in Tris-buffered saline containing 0.05% Tween 20 and 1% BSA or 5% nonfat dry milk and probed with appropriate antibodies (anti-IRS-1, anti-pTyr, anti-p85α). After extensive washing, the membranes were incubated with horseradish peroxidase-conjugated secondary antibodies and again washed, and then the protein bands were visualized by the enhanced chemiluminescence (ECL) method on a Lumi Imager workstation (Boehringer, Mannheim, Germany). All blots were quantified using the Lumi Imager software. The significance of reported differences was evaluated by using the null hypothesis and *t* statistics for unpaired data. A *p* value less than 0.05 was considered to be statistically significant.

Phosphopeptide Mapping by High-Performance Liquid Chromatography (HPLC) and Electrospray Ionization Mass Spectrometry (ESI-MS). Using 50 units (40 μg) of PKC-ζ, 5 nmol of rIRS-1$^{449-664}$ protein was phosphorylated with 50 μM ATP plus 0.25 mCi/mL [γ-^{32}P]ATP for 60 min under the conditions described above. Proteins were separated by SDS−PAGE, and phosphorylated rIRS-1$^{449-664}$ was digested with 100 μg of trypsin in the excised gel pieces overnight at 30 °C. Peptides were eluted with 50 mM NH_4HCO_3 and 50% acetonitrile and separated on an anion-exchange column (Nucleogel SAX 1000-8/46, 50 × 4.6 mm; Macherey & Nagel, Düren, Germany) using the Beckman gold solvent delivery system. The HPLC flow rate was 0.5 mL/min. After injection of sample, the peptides were eluted beginning at 100% of buffer A (20 mM NH_4CH_3COOH, pH 7.0) and 0% of buffer B (1 M KH_2PO_4, pH 4.0). The amount of buffer B was increased to 10% within 40 min and from 10% to 50% during the following 75 min. Fractions of 0.5 mL were collected, and radioactivity was measured by Cerenkov counting. Radioactive fractions were subjected to reversed-phase HPLC. Peptides were separated on a C18 reversed-phase column (Nucleosil 300-5 C18, 250 mm × 2 mm, 5 μm particle size, 300 Å pore size; Macherey & Nagel, Düren, Germany). The HPLC flow rate was adjusted to 0.33 mL/min. After application of the sample, elution started with 100% of solution A (0.1% TFA) and 0% of solution B [acetonitrile/TFA (84/0.1 v/v)]. The content of solution B was raised to 100% in 120 min. Again the radioactivity of the collected fractions was measured. Fractions containing radiolabeled peptides were subjected to ESI-TOF mass spectrometry. Mass spectra were recorded on an electrospray quadrupole time-of-flight mass spectrometer (QSTAR Pulsar I; Applied Biosystems, Foster City, CA) using a nanospray source (Protana, Odense, Denmark). Selected peptides were analyzed in tandem mass spectrometry mode, and the sequence and posttranslational modifications were retrieved by manual interpretation.

Site-Directed Mutagenesis. The serine 570 to alanine, serine 612 to alanine, and serine 498 to alanine mutants of rIRS-1$^{449-664}$ were generated by site-directed mutagenesis

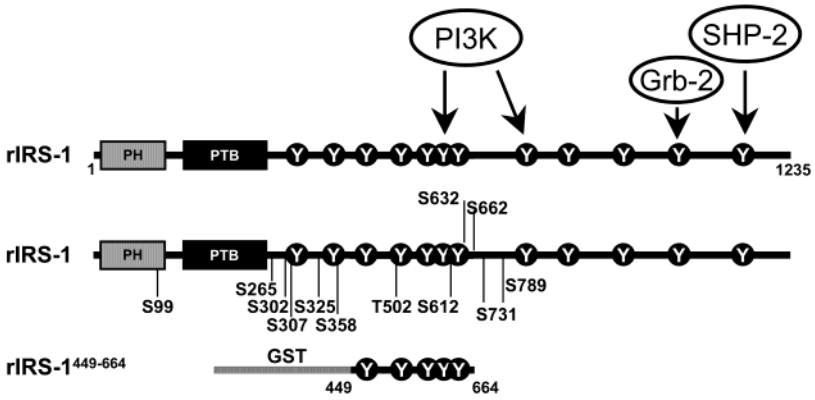

FIGURE 1: Schematic overview of IRS-1 with known interaction partners and known serine/threonine phosphorylation sites. Upper panel: The relative positions of the pleckstrin homology (PH) and phosphotyrosine-binding (PTB) domain are indicated, followed by a C-terminal tail that contains numerous tyrosine phosphorylation sites. Potential binding partners including PI 3-kinase, Grb2, and SHP-2 are also shown. Middle panel: Known (S307, S612, S632, S789) and potential serine phosphorylation sites are highlighted. Bottom panel: Construction of a GST fusion protein containing amino acids 449−664 of rat IRS-1 including the major binding site of the PI 3-kinase.

using the QuikChange site-directed mutagenesis kit according to the manufacturer's instructions using pGEX-5X-3/rIRS-$1^{449-664}$ as a template. The following primers were used: S570A, 5′-CCCGGCTACCGGCAT**GCC**GCCTTCGTGCCCACC and 3′-GGGCCGATGGCCGTA**CGG**CGGAAGCACGGGTGG; S612A, 5′-GGCTACATGCCCATG**GCT**CCCGGAGTGGCTCC and 3′-CCGATGTACGGGTAC**CGA**GGGCCTCACCGAGG; S498A, 5′-GGTGCTACCATGGGGACA**GCC**CCGGCGCTGACTGGAGAC and 3′-CCACGATGGTACCCCTGT**CGG**GGCCGCGACTGACCTCTG. The presence of the desired mutations was confirmed by sequencing the recombinant molecules by Qiagen Sequencing Services (Hilden, Germany).

Interaction Studies by Surface Plasmon Resonance Technology. The principle of operation of the BIAcore biosensor (Biacore, Freiburg, Germany) has been described previously (*42*). To avoid the interfering dimerization of the GST part of the fusion protein, it was cleaved with thrombin during the purification. Because of the known extremely fast association rates of SH2 domains to phosphopeptides, the relative affinities were assessed by competition assay (*43*). Therefore, a constant concentration of p85α (100 nM) was incubated in running buffer [0.01 M Hepes, pH 7.4, 0.15 M NaCl, 3 mM EDTA, 0.005% surfactant P20 (HBS-EP)] with a variable concentration of the competitor peptide (50 nM−10 μM), which was identical to that bound on the CM5 sensor chip surface. After a 1 h preincubation at room temperature the various mixtures were then injected sequentially at a flow rate of 5 μL/min at 25 °C in HBS-EP buffer. The peptides used, DDGYMPMSPGV, DDGpYMPMSPGV, DDGYMPMpSPGV, and DDGpYMPMpSPGV, representing amino acids 605−615 of rat IRS-1, were synthesized on an Applied Biosystems model 433 peptide synthesizer. All peptides were immobilized with a concentration of 5 mg/mL in 100 mM H_3BO_4 (NaOH, pH 8.5) at 1 μL/min by the standard amine coupling procedure as described by the manufacturer. Regeneration after each binding experiment was performed by injection of 6 M guanidine hydrochloride for 2 min. The kinetic analysis of the p85α with pY608 and pY606-pS612 interaction has been performed using the BIAevaluation 3.1 software (Biacore, Freiburg, Germany) and GraphPad Prism 3.0 (San Diego, CA).

RESULTS

An IRS-1 Domain Is Phosphorylated by the Insulin Receptor and Interacts with PI 3-Kinase. To determine the effects of serine/threonine phosphorylation of IRS-1 on the interaction with PI 3-kinase, we developed an in vitro phosphorylation and PI 3-kinase interaction assay using recombinant p85α and a GST pull-down approach. A selected part of the rat IRS-1 protein was cloned, expressed as a GST fusion protein, and purified from *E. coli*. This GST fusion protein (rIRS-$1^{449-664}$) covers a domain of 216 amino acids (449−664) of the rat IRS-1 protein containing potential tyrosine phosphorylation sites within YMXM or YXXM consensus motifs, including the major PI 3-kinase binding sites Tyr^{608} and Tyr^{628} (*39*) (see Figure 1). On the basis of the structure of the coded fusion protein a molecular mass of 51.2 kDa was calculated, and an apparent mass of 55 kDa was determined by SDS−PAGE. The experimental procedure of the in vitro phosphorylation and p85α interaction assay is outlined in Figure 2A. Exposing the fusion protein to WGA-purified insulin receptor induced a prominent insulin-stimulated tyrosine phosphorylation of rIRS-$1^{449-664}$ (Figure 2B, upper panel). Quantification showed an 8.8 ± 1.1-fold stimulation over basal (n = 10, Figure 2C). The GST pull-down assay revealed a significant increase in the interaction of the p85α regulatory subunit of PI 3-kinase with the tyrosine-phosphorylated rIRS-$1^{449-664}$ (Figure 2B, middle panel).

Different PKC Isoforms Inhibit Insulin-Stimulated Tyrosine Phosphorylation of rIRS-$1^{449-664}$ and Subsequent Association to p85α. To assess if protein kinase C is capable of phosphorylating rIRS-$1^{449-664}$ in vitro, we first incubated the fusion protein with PKC from rat brain (PKC-rb) and PKC-ζ in the presence of [^{32}P]ATP. rIRS-$1^{449-664}$ was then analyzed by SDS−PAGE and autoradiography (Figure 3A), and a prominent phosphorylation of rIRS-$1^{449-664}$ by PKC became detectable. rIRS-$1^{449-664}$ incubated with the same amount of PKC in the presence of PKC inhibitors exhibited no significant incorporation of phosphate (Figure 3A). A dose−response curve with increasing amounts of PKC was then determined to establish conditions of maximum phosphorylation, which was observed with 0.5 μg of PKC rat brain or PKC-ζ (data not shown). Using this condition we then

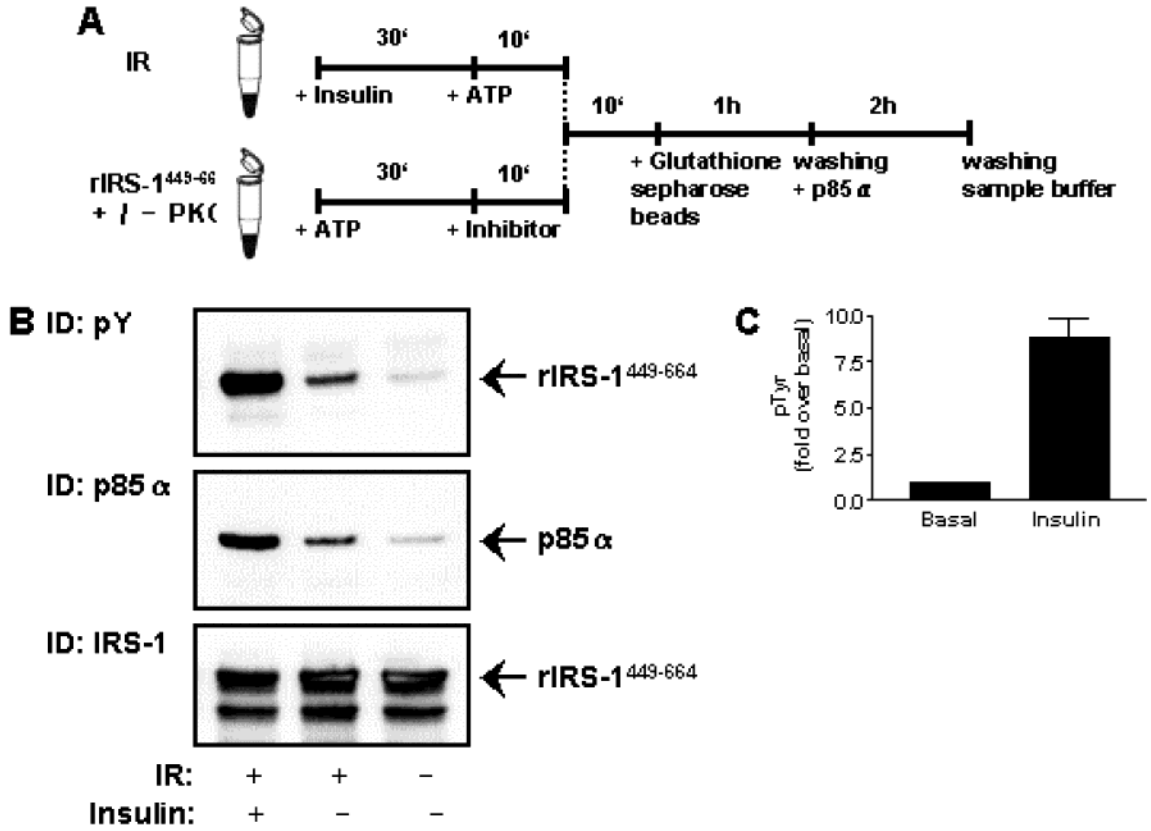

FIGURE 2: Tyrosine phosphorylation of rIRS-1$^{449-664}$ and interaction with the p85α subunit of PI 3-kinase. (A) Schematic diagram of the experimental procedure. 5 μg of IR was autophosphorylated for 10 min at 30 °C in phosphorylation buffer after a 30 min preincubation with 100 nM insulin. Substrate phosphorylation was subsequently initiated by addition of autophosphorylated IR to aliquots of 1 μg of rIRS-1$^{449-664}$, which was preincubated for 30 min in the absence or presence of PKC followed by addition of PKC inhibitor. The reaction proceeded for 10 min, then glutathione−Sepharose beads were added, and samples were incubated at 4 °C on a rotator for 1 h. Pellets were washed three times with binding buffer, 0.5 μg of recombinant p85α was added, and incubation was continued for 2 h. After washing, bound proteins were eluted by addition of 2× sample buffer followed by boiling for 5 min. (B) Eluted proteins were resolved by SDS−PAGE and were analyzed by immunoblotting using antibodies against phosphotyrosine, p85α and IRS-1, as detailed in Experimental Procedures. Representative blots out of six separate experiments are shown. (C) Quantification of rIRS-1$^{449-664}$ tyrosine phosphorylation was obtained using Lumi Imager software. Data are mean values ± SEM (n = 10).

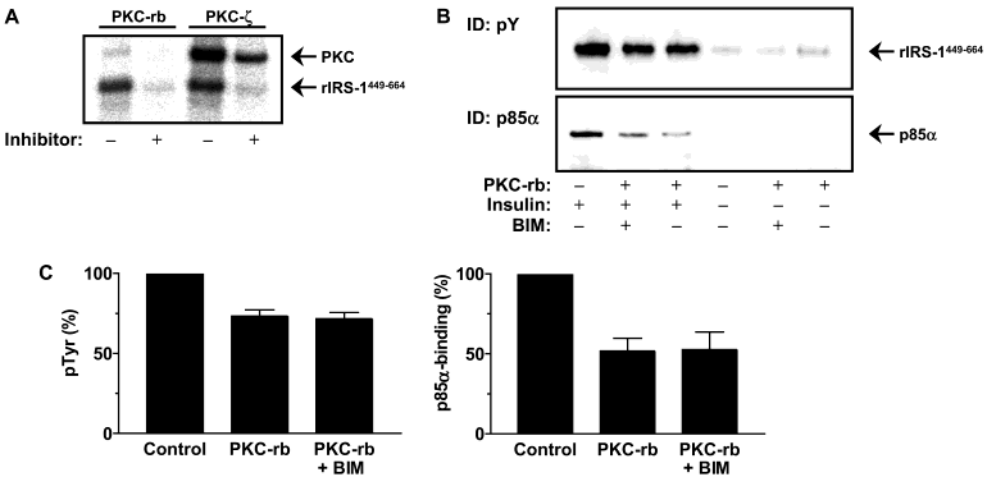

FIGURE 3: Effect of PKC from rat brain on tyrosine phosphorylation of rIRS-1$^{449-664}$ and interaction with p85α. (A) 1 μg of rIRS-1$^{449-664}$ was incubated with 0.5 μg of PKC from rat brain (PKC-rb) or 0.5 μg of PKC-ζ in the presence of 2 μCi of [^{32}P]ATP (final concentration 50 μM), as detailed in Experimental Procedures. The reaction was inhibited by 1 μM bisindolylmaleimide I (BIM) or 400 μM pseudosubstrate peptide for PKC-rb or PKC-ζ, respectively. Proteins were resolved by SDS−PAGE and subjected to autoradiography. (B) Tyrosine phosphorylation of rIRS-1$^{449-664}$ by IR and interaction with p85α were determined as described in Figure 2. rIRS-1$^{449-664}$ was preincubated with 0.5 μg of PKC-rb for 30 min. Representative blots are shown. When present, BIM was added for 10 min before starting substrate phosphorylation by IR (see Figure 2). (C) Quantification of the inhibitory effect of PKC-rb on insulin-stimulated tyrosine phosphorylation and p85α interaction with the insulin-stimulated value set as 100%. Data are mean values ± SEM (n = 6−9).

investigated the influence of the serine phosphorylation of rIRS-1$^{449-664}$ on the subsequent tyrosine phosphorylation by the autophosphorylated IR. Therefore, rIRS-1$^{449-664}$ was treated with or without PKC and then incubated with WGA-

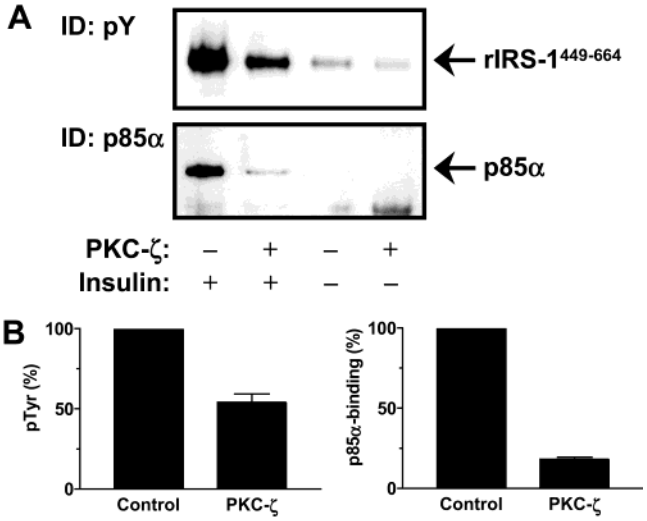

FIGURE 4: Effect of PKC-ζ on tyrosine phosphorylation of rIRS-$1^{449-664}$ and interaction with p85α. (A) rIRS-$1^{449-664}$ was preincubated with PKC-ζ (0.5 μg) for 30 min. Tyrosine phosphorylation by IR and interaction with p85α were determined by immunoblotting as detailed in Figure 2. (B) Quantification of the inhibitory effect of PKC-ζ was performed as described in Figure 3. Data are mean values ± SEM ($n = 3$).

purified IR. p85α association was subsequently determined by coupling rIRS-$1^{449-664}$ to glutathione−Sepharose beads via its GST part and incubation with 0.5 μg of p85α, as outlined in Figure 2A. Samples were analyzed by SDS−PAGE and immunoblotting with antibodies against phosphotyrosine (pTyr), p85α, and IRS-1. As shown in Figure 3B, pretreatment of rIRS-$1^{449-664}$ with PKC rat brain caused a decrease in the insulin-stimulated tyrosine phosphorylation and the interaction with p85α. Tyr phosphorylation of rIRS-$1^{449-664}$ was reduced by 27 ± 4% ($n = 9$) with a more prominent inhibition of the association of p85α (49 ± 8%) (Figure 3C). Inhibition of PKC-rb after phosphorylation of rIRS-$1^{449-664}$ by addition of bisindolylmaleimide (BIM) did not modify this result (Figure 3C). The experimental approach described in Figure 3B was then repeated for PKC-ζ. When compared to PKC-rb, an even more prominent reduction in the tyrosine phosphorylation of rIRS-$1^{449-664}$ and interaction with p85α was observed (Figure 4A). Quantification of the data showed an inhibition of tyrosine phosphorylation by 46 ± 5% ($n = 3$) and a concomitant inhibition of p85α binding to IRS-1 by 81 ± 1% (Figure 4B).

To exclude effects of PKC at the level of IR, the autophosphorylation of the β-subunit was examined. No significant alteration of IR autophosphorylation became detectable when the autoactivated receptor was incubated for 10 min at 30 °C in the presence of PKC-rb or PKC-ζ when compared to controls (Figure 5A). In a second set of experiments the PKC was incubated with the autoactivated IR and then inhibited by addition of specific inhibitors, and finally rIRS-$1^{449-664}$ was added for 10 min as a substrate (Figure 5B). Quantification of the phosphotyrosine content of rIRS-$1^{449-664}$ after incubation of the IR with PKC-rb and subsequent inhibition with BIM resulted in 82 ± 7% ($p > 0.05$) compared to the control situation. Without inhibition of PKC-rb the phosphotyrosine content of rIRS-$1^{449-664}$ was decreased to 70 ± 17% ($n = 3$). Inactivation of PKC-ζ with the pseudosubstrate inhibitor resulted in a phospho level of 89 ± 9% ($p > 0.05$) compared to 55 ± 11% with the uninhibited PKC-ζ ($n = 3$). Thus, the PKC isoforms used here do not modify IR kinase activity under our experimental conditions.

Identification and Functional Analysis of IRS-1 Serine Phosphorylation Sites Targeted by PKC. Prior studies have indicated that negative regulation of insulin signaling by protein kinase C involves the mitogen-activated protein kinase and phosphorylation of serine 612 in IRS-1 (*26*). Serine 612 is localized in direct neighborhood to a major YMXM motif at Y608, which is described to be one of the main interaction sites for PI 3-kinase (*39*). We assessed modification of this site by PKC using a specific IRS-1 phosphoserine 612 antibody (αpS^{612}). After incubation with PKC from rat brain and PKC-ζ for 30 min at 30 °C, rIRS-$1^{449-664}$ was strongly immunoblotted with αpS^{612} (Figure 6A); inhibition of PKC with BIM clearly prevented the phosphorylation of this serine.

To characterize the influence of phosphoserine 612 of IRS-1 on the interaction with PI 3-kinase, the technique of surface plasmon resonance (SPR) was used. For this purpose peptides were synthesized with the sequence DDGYMPMSPGV representing amino acids 605−615 of rat IRS-1 and immobilized on a chip surface by standard amine coupling. It has been reported that fusion of SH2 domains to GST may affect their binding to phosphopeptides, leading to an overestimation of the binding affinity (*44*). Therefore, the GST part of the recombinant p85α fusion protein was cleaved. Binding of p85α to the peptides was studied by applying various concentrations of the purified p85α to a biosensor chip to which the peptides were coupled in different phosphorylation forms. These experiments showed that p85α only binds to the tyrosine-phosphorylated form of the peptide (Figure 6B,C), consistent with the literature (*45*).

We then determined the relative binding affinity of this reaction by monitoring the binding of 100 nM p85α to the peptides pY608 (DDG**pY**MPMSPGV) and pY608−pS612 (DDG**pY**MPM**pS**PGV) in the presence of competing soluble peptides (Figure 6D−F). Half-maximum inhibitory concentrations (IC_{50}) were obtained by plotting the SPR response 440 s after injection at equilibrium versus the log peptide concentration. Both peptides displayed a measurable binding activity (Figure 6D versus Figure 6E). Solubilized peptides inhibited binding of p85α to the immobilized peptides at micromolar concentrations. Complete inhibition was achieved at a peptide concentration of ∼10 μM. Fitting of the determined readings with an equation for two-site competition resulted in an IC_{50} for pY608 of 0.26 and 16.56 μmol/L ($r^2 = 0.9983$) and for pY608−pS612 of 0.15 and 2.88 μmol/L ($r^2 = 0.9989$). These data show that the peptide pY608−pS612 inhibited the binding of p85α with a better efficiency, indicating that the presence of a phosphoserine residue at position +4 of the phosphotyrosine even increases the affinity of the p85α SH2 domain for the IRS-1 phosphopeptide.

To identify additional PKC-ζ phosphorylation sites on rIRS-$1^{449-664}$ that might promote the inhibition of insulin-stimulated tyrosine phosphorylation in the in vitro system, rIRS-$1^{449-664}$ was incubated with PKC-ζ and separated by SDS−PAGE. ^{32}P-Phosphorylated rIRS-$1^{449-664}$ was digested with trypsin and extracted from the gel. The peptides

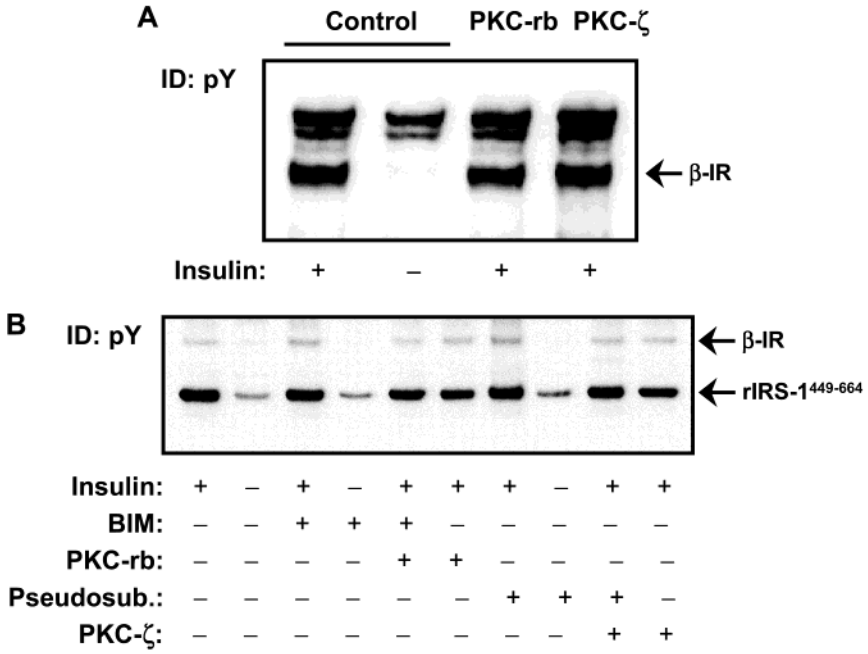

FIGURE 5: Effect of PKC isoforms on IR autophosphorylation and tyrosine kinase activity. (A) Autophosphorylation of IR was conducted as outlined in Figure 2. Either PKC-rb or PKC-ζ was added after 10 min of autophosphorylation, and incubation was continued for another 10 min. Tyrosine phosphorylation of the IR β-subunit was then analyzed by immunoblotting. (B) The experimental protocol was as outlined in (A) with the difference of addition of PKC inhibitors for 10 min after incubation of the autoactivated IR with PKC; then rIRS-1$^{449-664}$ was subsequently added for an additional 10 min. Tyrosine phosphorylation of rIRS-1$^{449-664}$ was then analyzed by immunoblotting (inhibitors: bisindolylmaleimide I for PKC-rb; pseudosubstrate peptide for PKC-ζ).

generated by digestion were resolved by two-dimensional HPLC, and the content of radioactivity in the fractions was monitored by Cerenkov counting. The HPLC profile of the first separation using an anion-exchange column showed six reproducible major peaks (Figure 7A). To separate comigrating peptides, radioactive fractions of each peak were pooled according to the elution profile and subjected to reversed-phase (RP) HPLC (Figure 7B). This resulted in ten distinct radiolabeled RP-HPLC fractions that were subsequently subjected to electrospray ionization mass spectrometry (ESI-MS). The results obtained by MS analysis are summarized in Table 1. Eight peptides could be identified, covering 37% of the rIRS-1$^{449-664}$ sequence. Two phosphoserines were found, Ser^{358} (Ser^{570} in full-length IRS-1) (LPGYRH**pS**AFVPTHSYPEEGLEMHHLER) in peak 4 of anion-exchange HPLC and Ser^{286} (Ser^{498} in IRS-1) (YIPGATMGT**pS**PALTGDEAAGAADLDNR) in peaks 5 and 6. Peak 4 containing Ser^{570} corresponded to about 19% of the incorporated radioactivity, whereas peaks 5 and 6 containing Ser^{498} accounted for 11% of the overall measured radioactivity.

Phosphoserine 358 was identified by ESI-MS/MS. The fragment ion with a mass difference of 97.9 Da to the parent ion indicates a phosphopeptide (Figure 8A). A mass difference of 97.9 Da correlates to the loss of phosphoric acid. The site of phosphorylation was identified by the loss of the phosphate group (HPO_3) and phosphoric acid (H_3PO_4) from the fragment ions b_9 and b_{10}. This dephosphorylation of the fragment ions indicates that the phosphorylation could only take place at Y355 or S358. S358 is the phosphoamino acid, because there was no dephosphorylation detected from the b_4 ion, indicating a phosphorylation at Y355 (data not shown).

Phosphoserine 612 could not be detected by mass spectrometry despite being detected by a phospho site-specific antibody (Figure 6A), but a peptide including this site was found in peak 2 together with three additional peptides. Peak 1 and peak 3 contained only one peptide covering 13% and 21% of the radioactivity, respectively (THSAGTSPTISHQK and TPSQSSVVSIEEYTEMMPAAYPPGGGSGGR). To further confirm that the phosphorylation sites found were Ser^{498}, Ser^{570}, and Ser^{612}, three additional GST fusion proteins with mutation of serine to alanine were generated. These GST fusion proteins were exposed to PKC-ζ and were phosphorylated by the enzyme at a level comparable to that of the wild type (data not shown). Mutation of Ser^{570} to alanine largely reduced peak 4 in anion-exchange HPLC (Figure 9B), demonstrating that Ser^{570} of IRS-1 is a novel phosphorylation site targeted by PKC-ζ. The Ser^{612} to alanine mutation leads to a decrease of peak 2 (Figure 9C), confirming the data obtained with the phospho-specific antiserum. Mutation of Ser^{498} to alanine resulted in a reduction of peaks 5 and 6 and an additional alteration of peak 2 (Figure 9D), supporting the data from mass spectrometry. Since Ser^{570} covers about 20% of the radioactivity incorporated into rIRS-1$^{449-664}$ in response to PKC-ζ, we generated a phospho-specific antiserum (αpS^{570}) against this site. After incubation with PKC-ζ for 30 min, rIRS-1$^{449-664}$ strongly immunoblotted with αpS^{570} with a 4−5-fold increase over basal (Figure 9E). This effect was completely blocked by the PKC-ζ pseudosubstrate and was undetectable in the S570A mutant of rIRS-1$^{449-664}$. Furthermore, PKC from rat brain was unable to phosphorylate rIRS-1$^{449-664}$ at position Ser^{570} (Figure 9E).

To determine the functional relevance of the identified phospho sites, the rIRS-1$^{449-664}$ Ser^{570} → Ala and Ser^{612} →

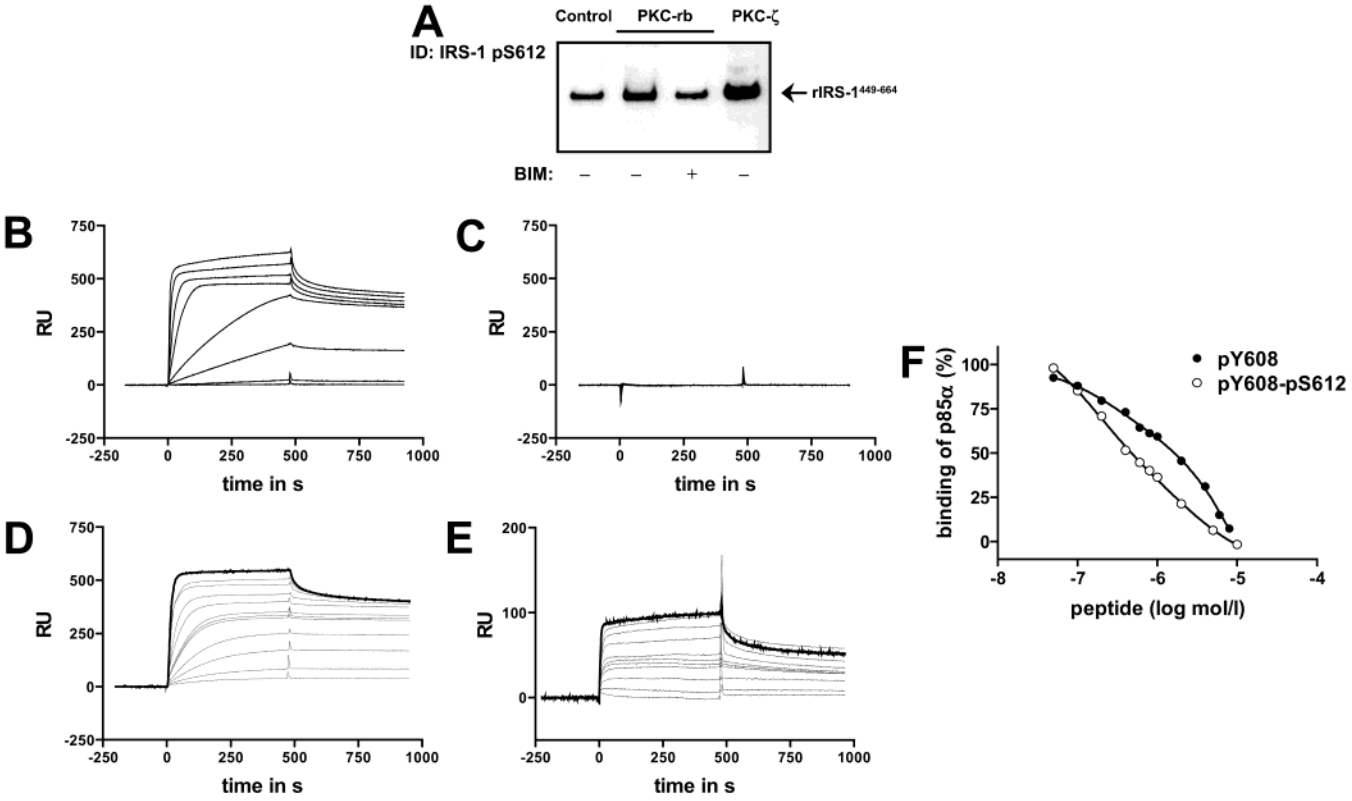

FIGURE 6: Identification of IRS-1 serine 612 as a target of PKC and interaction analysis with p85α using surface plasmon resonance. (A) 1 μg of rIRS-$1^{449-664}$ was incubated with 0.5 μg of the different PKCs for 30 min at 30 °C and immunoblotted with an antibody against phosphoserine 612. A representative experiment is shown. (B) Binding of p85α to immobilized peptides corresponding to IRS-1 amino acids 605−615 with phosphotyrosine 608 or (C) without phosphotyrosine using surface plasmon resonance (pY608, DDGpYMPMSPGV, and Y608, DDGYMPMSPGV). Protein concentrations of p85α used were (from bottom to top) 1, 5, 10, 25, 50, 100, 250, and 500 nM. (D) Inhibition of p85α binding by competition with soluble peptides pY608, DDG**pY**MPMSPGV, or (E) pY608−pS612, DDG**pY**MPM**pS**PGV. The soluble peptides were also immobilized on the chip. (F) Half-maximum inhibitory concentrations (IC_{50}) were obtained by plotting the SPR response at equilibrium (440 s after injection) versus the log peptide concentration. IC_{50}: for pY608, 0.26 and 16.56 μmol/L; for pY608−pS612, 0.15 and 2.88 μmol/L.

Ala mutants were tested in the in vitro phosphorylation and p85α interaction assay (Figure 10A). Comparing the results of tyrosine phosphorylation by IR after PKC-ζ pretreatment showed a comparable reduction (30−40%) for wild-type rIRS-$1^{449-664}$ and the two mutants (Figure 10B, left panel). However, a significant difference became apparent when the interaction of the two mutants was compared with p85α. Thus, p85α binding to S570A was reduced to 43 ± 4% (n = 3) of control by PKC-ζ treatment, with a reduction to 28 ± 3% for the S612A mutant of rIRS-$1^{449-664}$ (Figure 10B, right panel). No difference was observed between wild-type rIRS-$1^{449-664}$ and the S498A mutant (data not shown).

DISCUSSION

Serine phosphorylation of IRS-1 has been implicated as a negative regulator of insulin signal transduction (*16*−*19*, *21*, *32*, *34*). Recently, it was found that during insulin signaling IRS-1 is phosphorylated by the serine/threonine kinase PKC-ζ, thereby attenuating the insulin signal (*37*, *38*). Identification of IRS-1 serine/threonine phosphorylation sites involved in this process is an important step toward understanding the molecular mechanism of this negative feedback control in the insulin cascade. In the present study we have used an in vitro approach to identify serine/threonine phosphorylation sites for PKC-ζ within IRS-1 and to characterize the functional implications. We have developed an assay system using a GST-IRS-1 fragment as substrate and partially purified insulin receptor as the source of kinase. The chosen IRS-1 domain (rIRS-$1^{449-664}$) covers 216 amino acids and six of the YMXM or YXXM consensus motifs including Tyr^{608} and Tyr^{628}, which are of primary importance for full activation of PI 3-kinase and GLUT4 translocation (*39*). We show that direct interaction of PKC-ζ with rIRS-$1^{449-664}$ reduces its tyrosine phosphorylation by the insulin receptor, resulting in nearly complete abrogation of p85α binding to this IRS-1 domain. Taking advantage of our in vitro approach, we have identified Ser^{498} and Ser^{570} as two novel PKC-ζ phosphorylation sites in the vicinity of the PI 3-kinase binding domain. These data are consistent with the view that feedback control of IRS-1 function may involve Ser/Thr kinases downstream of PI 3-kinase (*27*, *34*, *46*) and support the notion (*37*, *38*) that PKC-ζ plays a major role in this process.

When we examined rIRS-$1^{449-664}$ as a potential substrate for PKC, we found that a mixture of conventional PKC isoforms (α, β_1, β_2, γ) purified from rat brain and the atypical isoform ζ were able to phosphorylate rIRS-$1^{449-664}$ under our in vitro conditions. In rat hepatoma Fao cells only PKC-ζ was found to induce Ser/Thr phosphorylation of IRS-1, with PKC-α, -δ, and -η being uneffective (*38*). However, the most recent data by Van Obberghen and co-workers (*47*) suggest that PKC-α may also promote this process, in agreement

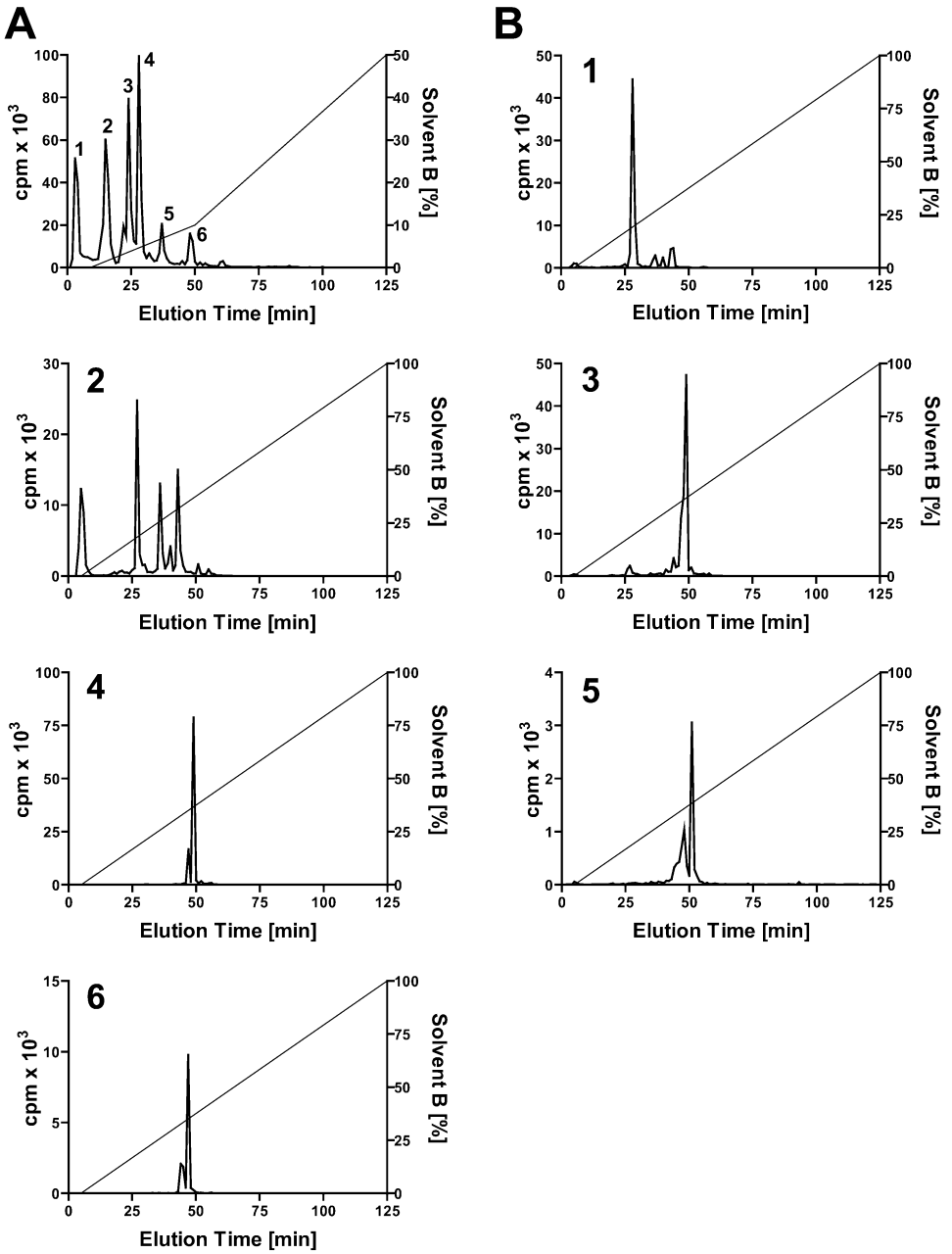

FIGURE 7: HPLC analysis of tryptic phosphopeptides derived from rIRS-1$^{449-664}$ phosphorylated by PKC-ζ. 5 nmol of rIRS-1$^{449-664}$ was phosphorylated for 60 min using 0.5 nmol of PKC-ζ and 50 μM ATP plus 0.25 mCi/mL [^{32}P]ATP, as described in Experimental Procedures. Proteins were separated by SDS−PAGE, and the excised rIRS-1$^{449-664}$ was digested with trypsin. The recovered ^{32}P-radiolabeled peptide mixture was separated by ion-exchange (A) and C18 reversed-phase HPLC (B). The radioactivity of the collected fractions was determined by Cerenkov counting. After reversed-phase HPLC radioactive fractions were analyzed by mass spectrometry.

with our in vitro findings. On the other hand, despite a comparable level of Ser/Thr phosphorylation of rIRS-1$^{449-664}$ by both classical PKC and PKC-ζ (see Figure 3), we observed a much more prominent inhibition of p85α association to the IRS-1 domain in response to PKC-ζ, making it likely that the functional implications of Ser/Thr phosphorylation of IRS-1 are more limited to PKC-ζ (*37*, *38*). Our data also show that PKC-ζ may modulate insulin signaling independent of phosphorylation at Ser^{307}. White and co-workers have shown that phosphorylation at this site inhibits the interaction of the phosphotyrosine-binding domain of IRS-1 with the phosphorylated motif in the activated insulin receptor (*24*). Interestingly, this site is also phosphorylated in response to insulin in muscle under in vivo conditions (*48*), and c-Jun N-terminal kinase (JNK) is thought to mediate this process (*16*, *30*). We conclude from our findings that Ser/Thr phosphorylation in the vicinity of the PI 3-kinase binding domain by PKC-ζ represents an additional way to mediate negative feedback regulation of insulin action.

Several studies have shown that PKC-α, -β_1, and -β_2 inhibit insulin signaling at the level of the insulin receptor itself (*49*−*51*), suggesting an additional complexity of the negative modulation of insulin action. In these studies the PKC isoforms were found to inhibit insulin receptor autophosphorylation and tyrosine kinase activity. In our in vitro experiments the insulin receptor was autophosphorylated before being exposed to PKC. Using this design, we clearly

Table 1: Sequence Analysis Results of rIRS-$1^{449-664}$ Phosphopeptides[a]

amino acid sequence of identified phosphopeptide	aa in rIRS-$1^{449-664}$ [b]	phosphorylated residue	peak[c]	part of ^{32}P (%)[d]
VAHTPPARGEEELSNYICMGGK	233−254		4 and 2	
GASTLTAPNGHYILSR	255−270		2	20.7
YIPGATMGT**S**PALTGDEAAGAADLDNR	277−303	S286	5 and 6	10.6
THSAGTSPTISHQK	308−321		1	12.9
TPSQSSVVSIEEYTEMMPAAYPPGGGSGGR	322−351		3	21.2
LPGYRH**S**AFVPTHSYPEEGLEMHHLER	352−378	S358	4	18.8
GGHHRPDSSNLHTDDGYMPMSPGVAPVPSNR	380−410		2	20.7
VDPNGYMMMSPSAAAS	441−456		2	20.7

[a] Tryptic peptides of rIRS-$1^{449-664}$ were analyzed after anion-exchange HPLC and reversed-phase HPLC by mass spectrometry. Phosphorylated serine residues are marked in bold letters. [b] Numbering was according to a composed sequence of glutathione *S*-transferase plus IRS-1 amino acids 449−664. [c] Peaks are from anion-exchange chromatography HPLC (numbers) (see Figure 7A). [d] The total amount of radioactivity incorporated into the identified phosphopeptides was set as 100%, and the percentage given represents the integrated peak area.

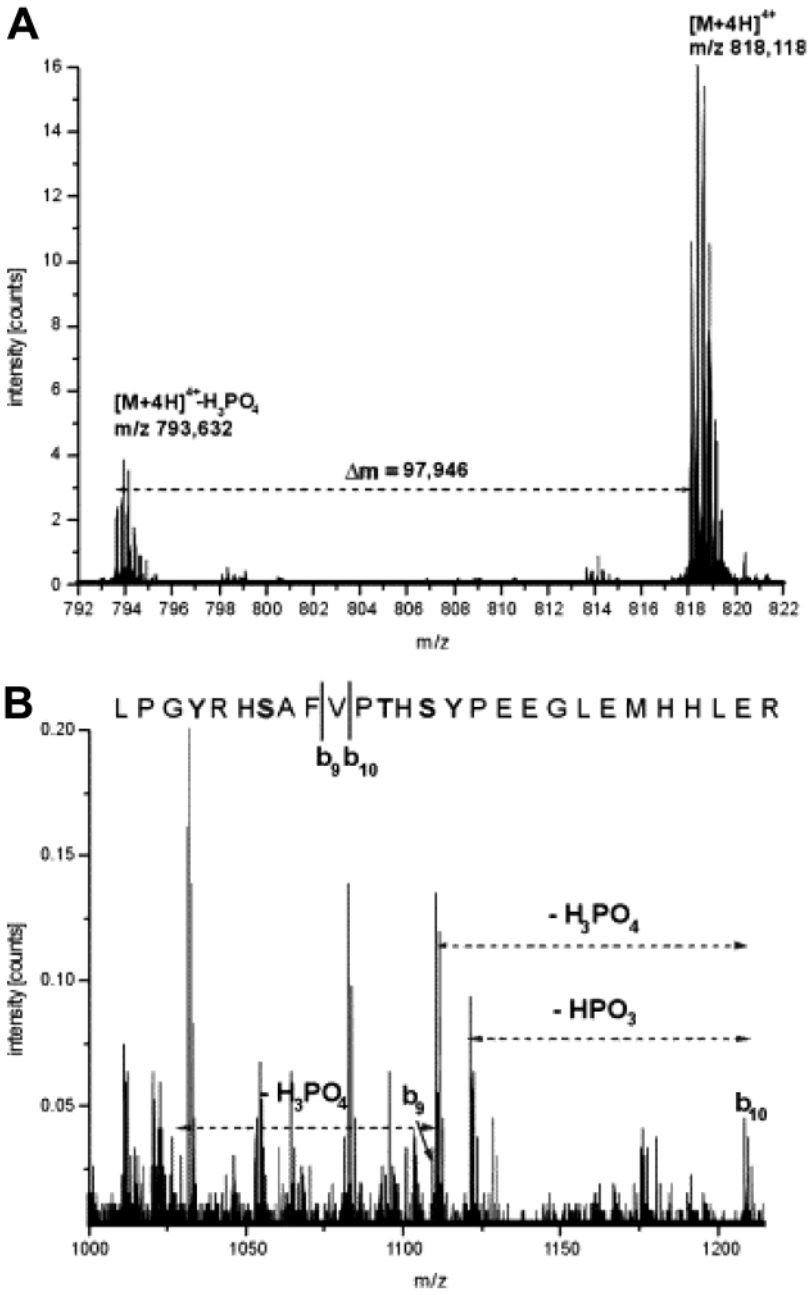

FIGURE 8: ESI-MS/MS spectra from the phosphopeptide 352−378. (A) Loss of phosphoric acid from the parent ion $[M + 4H]^{4+} = 818.11$, indicating the phosphorylation. (B) Dephosphorylation of the fragment ions b_9 and b_{10}, indicating the phosphorylation site.

ruled out any effect of PKC at the level of the insulin receptor, suggesting that autophosphorylation may protect the IR against desensitization by PKC. Future work should address this issue, specifically in a cellular context.

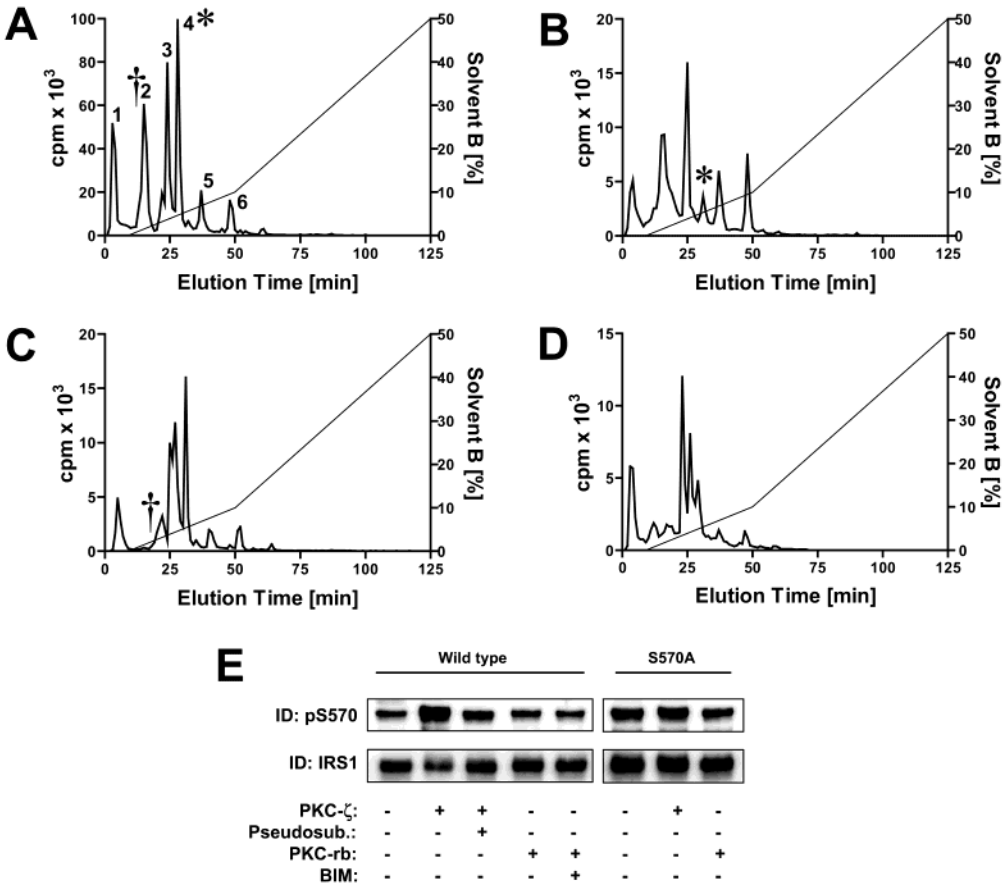

FIGURE 9: HPLC analysis of tryptic phosphopeptides of rIRS-1$^{449-664}$ and mutants S498A, S570A, and S612A. HPLC analysis of tryptic peptides generated from wild-type rIRS-1$^{449-664}$ (A), rIRS-1$^{449-664}$ S570A (B), rIRS-1$^{449-664}$ S612A (C), and rIRS-1$^{449-664}$ S498A (D) phosphorylated with recombinant PKC-ζ is shown. Representative HPLC profiles are presented. (E) 1 μg of rIRS-1$^{449-664}$ or IRS-1$^{449-664}$ S570A was incubated with the indicated PKC isoforms as detailed in Figure 6 and subsequently immunoblotted with an antiserum against phosphoserine 570. A representative experiment out of three is shown.

Using a commercially available antibody against IRS-1 phosphoserine 612, we found that the conventional PKC-α, -β_1, -β_2, and -γ and also the atypical isoform ζ are capable of transferring a phosphate group to this serine residue. Prior studies have indicated that this serine may participate in the negative regulation of insulin signaling by PKC, presumably by its close proximity to the YMPM***S*** consensus motif of tyrosine 608 (*33*). To characterize the influence of this serine on the interaction of tyrosine-phosphorylated IRS-1 with PI 3-kinase, surface plasmon resonance (SPR) technology was used. Binding of p85α to a 10mer phosphopeptide representing IRS-1 amino acids 605−615 was assessed in a competition assay. A similar approach has recently been used to study the binding of p85α wild type and mutants to tyrosine-phosphorylated peptides (*52*). Surprisingly, the affinity of p85α for the peptide appears to be even higher in the presence of phosphoserine 612 compared to the dephospho form. These data suggest that phosphorylation of Ser^{612} per se, although in the immediate vicinity of the PI 3-kinase binding site, is not sufficient to modify insulin signaling. This is consistent with more recent evidence showing that multiple Ser phosphorylation sites of IRS-1 (*32*) are targeted by multiple serine kinases (*53*), resulting in a highly complex regulation of IRS-1 activity.

To identify additional PKC phosphorylation sites, we analyzed tryptic peptides of rIRS-1$^{449-664}$ phosphorylated by PKC-ζ using a combination of two different sequential HPLC protocols coupled to ESI mass spectrometry. Using this approach, we identified Ser^{498} and Ser^{570} as novel PKC-ζ phosphorylation sites within IRS-1. Using a similar approach with the IRS-1 fragment IRS-1$^{265-522}$, very recently a major PKC-ζ phosphorylation site was identified at Ser^{318} (*56*). The functional implication of this site is not clear, but it could be similar to Ser^{307}, demonstrating again that multiple serine sites are involved in the regulation of IRS-1 activity. Mutation of Ser^{570} to alanine confirmed the MS results by strongly reducing peak 4 in the HPLC analysis. Since about 19% of the incorporated radioactivity can be attributed to Ser^{570}, this serine is one major phosphorylation site of PKC-ζ in rIRS-1$^{449-664}$. The peptide found in peak 3 accounted for 21% of the radioactivity and therefore might include a second major site. However, no phosphorylation could be detected by mass spectrometry, and preliminary mutation analysis did not reveal the responsible site. A conventional consensus phosphorylation motif for PKC was determined to be RXXS/TXRX, where X indicates any amino acid (*54*), but it has not proven robust or specific for all PKC isoenzymes (*55*). An optimal PKC-ζ consensus motif based upon screening of a peptide library (*55*) showed that PKC-ζ selected for substrates with basic residues at positions −6, −4, and −2 of the phospho site but was not as selective for basic residues at postitions +2 and +3. Instead, peptides with hydrophobic residues at these positions were usually selected. Interestingly, the identified PKC-ζ phosphorylation site Ser^{570}

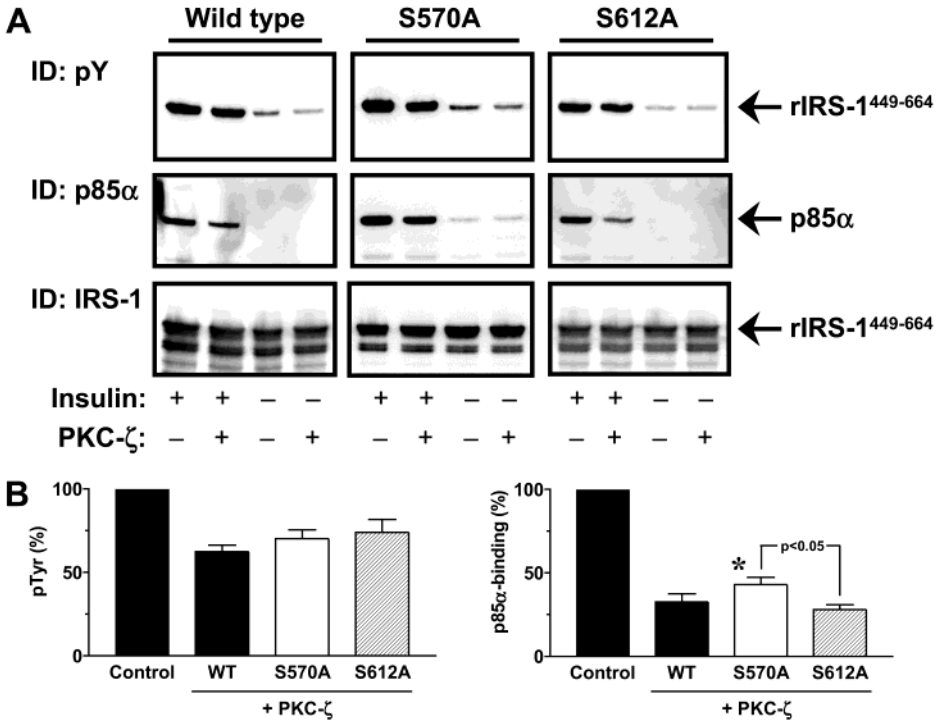

FIGURE 10: Functional analysis of Ser^{570} and Ser^{612}. (A) rIRS-$1^{449-664}$ and the indicated mutants were preincubated in the absence or presence of PKC-ζ and subjected to tyrosine phosphorylation by IR and interaction with p85α, as outlined in Figure 3. Representative Western blots are shown. (B) Blots were quantified using Lumi Imager software, and data are expressed relative to the insulin-stimulated control value set as 100%. Control data were obtained with wild-type and mutant IRS-1 fragments in the absence of PKC-ζ. Results are mean values ± SEM ($n = 3$). The asterisk indicates not significantly different from wild type ($p > 0.05$)

corresponds quite well with the described consensus motif (PGYRH**pS**AFVPT). On the other hand, the amino acid sequences surrounding serine 498 (ATMGT**pS**PALTG) and serine 612 (GYMPM**pS**PGVAP) do not fit to either the general PKC consensus motif or the optimal PKC-ζ consensus motif. It is worth noting that Ser^{570} exists in highly conserved motifs among all known IRS-1 homologues of different species. Importantly, by generating an antiserum against phosphoserine 570 of IRS-1, we were able to demonstrate that this site is not targeted by PKC from rat brain. We therefore conclude that Ser^{570} represents a major phosphorylation site with potential implication for the modulation of insulin signaling by PKC-ζ.

Functional analysis of the rIRS-$1^{449-664}$ Ser^{612} → Ala mutant indicated that this site does not mediate the inhibitory action of PKC-ζ on Tyr phosphorylation and association to p85α. This is consistent with our results obtained with surface plasmon resonance and the functional analysis of this site in cellular systems (*32*). A different result was observed for the Ser^{570} → Ala mutant, which exhibited improved interaction with p85α despite an unaltered reduction in tyrosine phosphorylation. It may be speculated that Ser^{570} plays a role in the inhibition of the p85α SH2 domain binding to the phosphotyrosine motif in IRS-1. This would be similar to the functional role of Ser^{307}, which inhibits binding of IRS-1 to the phosphorylated insulin receptor (*24*). However, mutation of Ser^{570} only partially rescued the association of p85α to the IRS-1 fragment, and this did not reach statistical significance when compared to the wild type. This may reflect the limitations of our in vitro model and/or the involvement of additional phospho sites in this process. The functional analysis of Ser^{570} of IRS-1 in intact cells is currently under way in our laboratory.

In summary, our data show that PKC-ζ exerts a strong negative control on insulin signaling at the level of IRS-1/PI 3-kinase interaction. Ser^{498} and Ser^{570} of IRS-1 have been identified as two novel phosphorylation sites for PKC-ζ, with Ser^{570} representing a major site with potential functional implications specifically targeted by PKC-ζ. These results emphasize the central role of PKC-ζ for negative feedback control of insulin signaling and will allow a more detailed analysis of this pathway under normal and pathophysiological conditions.

REFERENCES

1. White, M. F. (1998) The IRS-signalling system: A network of docking proteins that mediate insulin action, *Mol. Cell. Biochem. 182*, 3−11.
2. Cheatham, B., and Kahn, C. R. (1995) Insulin action and the insulin signaling network, *Endocr. Rev. 16*, 117−142.
3. Backer, J. M., Myers, M. G., Jr., Shoelson, S. E., Chin, D. J., Sun, X. J., Miralpeix, M., Hu, P., Margolis, B., Skolnik, E. Y., and Schlessinger, J. (1992) Phosphatidylinositol 3′-kinase is activated by association with IRS-1 during insulin stimulation, *EMBO J. 11*, 3469−3479.
4. Skolnik, E. Y., Lee, C. H., Batzer, A., Vicentini, L. M., Zhou, M., Daly, R., Myers, M. J., Jr., Backer, J. M., Ullrich, A., and White, M. F. (1993) The SH2/SH3 domain-containing protein GRB2 interacts with tyrosine-phosphorylated IRS1 and Shc: implications for insulin control of ras signaling, *EMBO J. 12*, 1929−1936.
5. Sun, X. J., Crimmins, D. L., Myers, M. G., Jr., Miralpeix, M., and White, M. F. (1993) Pleiotropic insulin signals are engaged by multisite phosphorylation of IRS-1, *Mol. Cell. Biol. 13*, 7418−7428.
6. Shepherd, P. R., Withers, D. J., and Siddle, K. (1998) Phosphoinositide 3-kinase: the key switch mechanism in insulin signalling, *Biochem. J. 333*, 471−490.
7. Alessi, D. R., and Cohen, P. (1998) Mechanism of activation and function of protein kinase B, *Curr. Opin. Genet. Dev. 8*, 55−62.

8. Lawlor, M. A., and Alessi, D. R. (2001) PKB/Akt: a key mediator of cell proliferation, survival and insulin responses?, *J. Cell. Sci. 114*, 2903−2910.
9. Bandyopadhyay, G., Sajan, M. P., Kanoh, Y., Standaert, M. L., Quon, M. J., Reed, B. C., Dikic, I., and Farese, R. V. (2001) Glucose activates protein kinase C-zeta /lambda through proline-rich tyrosine kinase-2, extracellular signal-regulated kinase, and phospholipase D: a novel mechanism for activating glucose transporter translocation, *J. Biol. Chem. 276*, 35537−35545.
10. Bandyopadhyay, G., Sajan, M. P., Kanoh, Y., Standaert, M. L., Quon, M. J., Lea-Currie, R., Sen, A., and Farese, R. V. (2002) PKC-zeta mediates insulin effects on glucose transport in cultured preadipocyte-derived human adipocytes, *J. Clin. Endocrinol. Metab. 87*, 716−723.
11. Summers, S. A., Kao, A. W., Kohn, A. D., Backus, G. S., Roth, R. A., Pessin, J. E., and Birnbaum, M. J. (1999) The role of glycogen synthase kinase 3beta in insulin-stimulated glucose metabolism, *J. Biol. Chem. 274*, 17934−17940.
12. Kitamura, T., Kitamura, Y., Kuroda, S., Hino, Y., Ando, M., Kotani, K., Konishi, H., Matsuzaki, H., Kikkawa, U., Ogawa, W., and Kasuga, M. (1999) Insulin-induced phosphorylation and activation of cyclic nucleotide phosphodiesterase 3B by the serine-threonine kinase Akt, *Mol. Cell. Biol. 19*, 6286−6296.
13. Eriksson, H., Ridderstrale, M., Degerman, E., Ekholm, D., Smith, C. J., Manganiello, V. C., Belfrage, P., and Tornqvist, H. (1995) Evidence for the key role of the adipocyte cGMP-inhibited cAMP phosphodiesterase in the antilipolytic action of insulin, *Biochim. Biophys. Acta 1266*, 101−107.
14. Nave, B. T., Ouwens, M., Withers, D. J., Alessi, D. R., and Shepherd, P. R. (1999) Mammalian target of rapamycin is a direct target for protein kinase B: identification of a convergence point for opposing effects of insulin and amino acid deficiency on protein translation, *Biochem. J. 344*, 427−431.
15. Scott, P. H., Brunn, G. J., Kohn, A. D., Roth, R. A., and Lawrence, J. C., Jr. (1998) Evidence of insulin-stimulated phosphorylation and activation of the mammalian target of rapamycin mediated by a protein kinase B signaling pathway, *Proc. Natl. Acad. Sci. U.S.A. 95*, 7772−7777.
16. White, M. F. (2002) IRS proteins and the common path to diabetes, *Am. J. Physiol. 283*, E413−E422.
17. Birnbaum, M. J. (2001) Turning down insulin signaling, *J. Clin. Invest. 108*, 655−659.
18. Zick, Y. (2001) Insulin resistance: a phosphorylation-based uncoupling of insulin signaling, *Trends Cell Biol. 11*, 437−441.
19. Tanti, J. F., Gremeaux, T., van Obberghen, E., and Le Marchand-Brustel, Y. (1994) Serine/threonine phosphorylation of insulin receptor substrate 1 modulates insulin receptor signaling, *J. Biol. Chem. 269*, 6051−6057.
20. Sun, X. J., Rothenberg, P., Kahn, C. R., Backer, J. M., Araki, E., Wilden, P. A., Cahill, D. A., Goldstein, B. J., and White, M. F. (1991) Structure of the insulin receptor substrate IRS-1 defines a unique signal transduction protein, *Nature 352*, 73−77.
21. Hotamisligil, G. S., Peraldi, P., Budavari, A., Ellis, R., White, M. F., and Spiegelman, B. M. (1996) IRS-1-mediated inhibition of insulin receptor tyrosine kinase activity in TNF-alpha- and obesity-induced insulin resistance, *Science 271*, 665−668.
22. Shulman, G. I. (2000) Cellular mechanisms of insulin resistance, *J. Clin. Invest. 106*, 171−176.
23. Virkamaki, A., Ueki, K., and Kahn, C. R. (1999) Protein−protein interaction in insulin signaling and the molecular mechanisms of insulin resistance, *J. Clin. Invest. 103*, 931−943.
24. Aguirre, V., Werner, E. D., Giraud, J., Lee, Y. H., Shoelson, S. E., and White, M. F. (2002) Phosphorylation of Ser307 in insulin receptor substrate-1 blocks interactionsm with the insulin receptor and inhibits insulin action, *J. Biol. Chem. 277*, 1531−1537.
25. Gao, Z., Hwang, D., Bataille, F., Lefevre, M., York, D., Quon, M. J., and Ye, J. (2002) Serine phosphorylation of insulin receptor substrate 1 by inhibitor kappa B kinase complex, *J. Biol. Chem. 277*, 48115−48121.
26. De Fea, K., and Roth, R. A. (1997) Modulation of insulin receptor substrate-1 tyrosine phosphorylation and function by mitogen-activated protein kinase, *J. Biol. Chem. 272*, 31400−31406.
27. Paz, K., Liu, Y. F., Shorer, H., Hemi, R., LeRoith, D., Quan, M., Kanety, H., Seger, R., and Zick, Y. (1999) Phosphorylation of insulin receptor substrate-1 (IRS-1) by protein kinase B positively regulates IRS-1 function, *J. Biol. Chem. 274*, 28816−28822.
28. Jakobsen, S. N., Hardie, D. G., Morrice, N., and Tornqvist, H. E. (2001) 5′-AMP-activated protein kinase phosphorylates IRS-1 on Ser-789 in mouse C2C12 myotubes in response to 5-aminoimidazole-4-carboxamide riboside, *J. Biol. Chem. 276*, 46912−46916.
29. Greene, M. W., and Garofalo, R. S. (2002) Positive and negative regulatory role of insulin receptor substrate 1 and 2 (IRS-1 and IRS-2) serine/threonine phosphorylation, *Biochemistry 41*, 7082−7091.
30. Lee, Y. H., Giraud, J., Davis, R. J., and White, M. F. (2003) c-Jun N-terminal kinase (JNK) mediates feedback inhibition of the insulin signaling cascade, *J. Biol. Chem. 278*, 2896−2902.
31. Qiao, L. Y., Zhande, R., Jetton, T. L., Zhou, G., and Sun, X. J. (2002) In vivo phosphorylation of insulin receptor substrate 1 at serine 789 by a novel serine kinase in insulin-resistant rodents, *J. Biol. Chem. 277*, 26530−26539.
32. Mothe, I., and Van Obberghen, E. (1996) Phosphorylation of insulin receptor substrate-1 on multiple serine residues, 612, 632, 662, and 731, modulates insulin action, *J. Biol. Chem. 271*, 11222−11227.
33. DeFea, K., and Roth, R. A. (1997) Protein kinase C modulation of insulin receptor substrate-1 tyrosine phosphorylation requires serine 612, *Biochemistry 36*, 12939−12947.
34. Li, J., DeFea, K., and Roth, R. A. (1999) Modulation of Insulin Receptor Substrate-1 Tyrosine Phosphorylation by an Akt/Phosphatidylinositol 3-Kinase Pathway, *J. Biol. Chem. 274*, 9351−9356.
35. Braiman, L., Alt, A., Kuroki, T., Ohba, M., Bak, A., Tennenbaum, T., and Sampson, S. R. (2001) Activation of protein kinase C zeta induces serine phosphorylation of VAMP2 in the GLUT4 compartment and increases glucose transport in skeletal muscle, *Mol. Cell. Biol. 21*, 7852−7861.
36. Standaert, M. L., Ortmeyer, H. K., Sajan, M. P., Kanoh, Y., Bandyopadhyay, G., Hansen, B. C., and Farese, R. V. (2002) Skeletal muscle insulin resistance in obesity-associated type 2 diabetes in monkeys is linked to a defect in insulin activation of protein kinase C-zeta/lambda/iota, *Diabetes 51*, 2936−2943.
37. Ravichandran, L. V., Esposito, D. L., Chen, J., and Quon, M. J. (2001) Protein kinase C-zeta phosphorylates insulin receptor substrate-1 and impairs its ability to activate phosphatidylinositol 3-kinase in response to insulin, *J. Biol. Chem. 276*, 3543−3549.
38. Liu, Y. F., Paz, K., Herschkovitz, A., Alt, A., Tennenbaum, T., Sampson, S. R., Ohba, M., Kuroki, T., LeRoith, D., and Zick, Y. (2001) Insulin stimulates PKCzeta-mediated phosphorylation of insulin receptor substrate-1 (IRS-1). A self-attenuated mechanism to negatively regulate the function of IRS proteins, *J. Biol. Chem. 276*, 14459−14465.
39. Esposito, D. L., Li, Y., Cama, A., and Quon, M. J. (2001) Tyr(612) and Tyr(632) in human insulin receptor substrate-1 are important for full activation of insulin-stimulated phosphatidylinositol 3-kinase activity and translocation of GLUT4 in adipose cells, *Endocrinology 142*, 2833−2840.
40. Smith, D. B., and Johnson, K. S. (1988) Single-step purification of polypeptides expressed in *Escherichia coli* as fusions with glutathione S-transferase, *Gene 67*, 31−40.
41. Burant, C. F., Treutelaar, M. K., Landreth, G. E., and Buse, M. G. (1984) Phosphorylation of insulin receptors solubilized from rat skeletal muscle, *Diabetes 33*, 704−708.
42. Malmqvist, M., and Karlsson, R. (1997) Biomolecular interaction analysis: affinity biosensor technologies for functional analysis of proteins, *Curr. Opin. Chem. Biol. 1*, 378−383.
43. Vely, F., Trautmann, A., and Vivier, E. (2000) BIAcore analysis to test phosphopeptide-SH2 domain interactions, *Methods Mol. Biol. 121*, 313−321.
44. Ladbury, J. E., Lemmon, M. A., Zhou, M., Green, J., Botfield, M. C., and Schlessinger, J. (1995) Measurement of the binding of tyrosyl phosphopeptides to SH2 domains: a reappraisal, *Proc. Natl. Acad. Sci. U.S.A. 92*, 3199−3203.
45. Felder, S., Zhou, M., Hu, P., Urena, J., Ullrich, A., Chaudhuri, M., White, M., Shoelson, S. E., and Schlessinger, J. (1993) SH2 domains exhibit high-affinity binding to tyrosine-phosphorylated peptides yet also exhibit rapid dissociation and exchange, *Mol. Cell. Biol. 13*, 1449−1455.
46. Eldar-Finkelman, H., and Krebs, E. G. (1997) Phosphorylation of insulin receptor substrate 1 by glycogen synthase kinase 3 impairs insulin action, *Proc. Natl. Acad. Sci. U.S.A. 94*, 9660−9664.
47. Miele, C., Riboulet, A., Maitan, M. A., Oriente, F., Romano, C., Formisano, P., Giudicelli, J., Beguinot, F., and Van Obberghen, E. (2003) Human glycated albumin affects glucose metabolism in L6 skeletal muscle cells by impairing insulin-induced insulin receptor substrate (IRS) signaling through a protein kinase C alpha-mediated mechanism, *J. Biol. Chem. 278*, 47376−47387.

48. Rui, L., Aguirre, V., Kim, J. K., Shulman, G. I., Lee, A., Corbould, A., Dunaif, A., and White, M. F. (2001) Insulin/IGF-1 and TNF-alpha stimulate phosphorylation of IRS-1 at inhibitory Ser307 via distinct pathways, *J. Clin. Invest. 107*, 181−189.
49. Bossenmaier, B., Mosthaf, L., Mischak, H., Ullrich, A., and Haring, H. U. (1997) Protein kinase C isoforms beta 1 and beta 2 inhibit the tyrosine kinase activity of the insulin receptor, *Diabetologia 40*, 863−866.
50. Strack, V., Hennige, A. M., Krutzfeldt, J., Bossenmaier, B., Klein, H. H., Kellerer, M., Lammers, R., and Haring, H. U. (2000) Serine residues 994 and 1023/25 are important for insulin receptor kinase inhibition by protein kinase C isoforms beta2 and theta, *Diabetologia 43*, 443−449.
51. Rosenzweig, T., Braiman, L., Bak, A., Alt, A., Kuroki, T., and Sampson, S. R. (2002) Differential effects of tumor necrosis factor-alpha on protein kinase C isoforms alpha and delta mediate inhibition of insulin receptor signaling, *Diabetes 51*, 1921−1930.
52. Baynes, K. C., Beeton, C. A., Panayotou, G., Stein, R., Soos, M., Hansen, T., Simpson, H., O'Rahilly, S., Shepherd, P. R., and Whitehead, J. P. (2000) Natural variants of human p85 alpha phosphoinositide 3-kinase in severe insulin resistance: a novel variant with impaired insulin-stimulated lipid kinase activity, *Diabetologia 43*, 321−331.
53. Gao, Z., Zuberi, A., Quon, M. J., Dong, Z., and Ye, J. (2003) Aspirin inhibits serine phosphorylation of insulin receptor substrate 1 in tumor necrosis factor-treated cells through targeting multiple serine kinases, *J. Biol. Chem. 278*, 24944−24950.
54. Pearson, R. B., and Kemp, B. E. (1991) Protein kinase phosphorylation site sequences and consensus specificity motifs: tabulations, *Methods Enzymol. 200*, 62−81.
55. Nishikawa, K., Toker, A., Johannes, F. J., Songyang, Z., and Cantley, L. C. (1997) Determination of the specific substrate sequence motifs of protein kinase C isozymes, *J. Biol. Chem. 272*, 952−960.
56. Beck, A., Moeschel, K., Deeg, M., Haring, H. U., Voelter, W., Schleicher, E. D., and Lehmann, R. (2003) Identification of an in vitro insulin receptor substrate-1 phosphorylation site by negative-ion muLC/ES-API-CID-MS hybrid scan technique, *J. Am. Soc. Mass. Spectrom. 14*, 401−405.

BI049640V